A new unconventional antiferromagnet, Yb_3Pt_4

M.C. Bennett [a,b,*], P. Khalifah [c,d], D.A. Sokolov [a,c], W.J. Gannon [a], Y. Yiu [a,b], M.S. Kim [a,c], C. Henderson [e], M.C. Aronson [a,b,c]

[a] Department of Physics, University of Michigan, Ann Arbor, MI 48109-1120, USA
[b] Department of Physics and Astronomy, Stony Brook University, Stony Brook, NY 11974, USA
[c] Brookhaven National Laboratory, Upton, NY 11973, USA
[d] Department of Chemistry, Stony Brook University, Stony Brook, NY 11974, USA
[e] Electron Microbeam Analysis Laboratory, University of Michigan, 48109-1005, USA

ARTICLE INFO

ABSTRACT

We report the synthesis and basic properties of single crystals of a new binary compound, Yb_3Pt_4. The Yb ions in this compound are fully trivalent, and heat capacity measurements show that the crystal field scheme involves a doublet ground state, well separated from the excited states, which are fully occupied above ~ 150 K. The heat capacity displays a large, weakly first order anomaly at 2.4 K, where a cusp is observed in the magnetic susceptibility signalling the onset of antiferromagnetic order. The entropy associated with this order is the full $R\ln 2$ of the doublet ground state, however, the magnetic susceptibility in the ordered phase is dominated by a large and temperature independent component below the Neel temperature. The heat capacity in the ordered state originates with ferromagnetic spin waves, giving evidence for the inherently local moment character of the ordered state. The electrical resistivity is unusually large, and becomes quadratic in temperature exactly at the Neel temperature. The absence of analogous Fermi liquid behavior in the heat capacity and the magnetic susceptibility implies that Yb_3Pt_4 is a low electron density system, where the Fermi surface is further gapped by the onset of magnetic order.

1. Introduction

Due in part to their ubiquity among different classes of strongly correlated systems, there is longstanding interest in the effects of quantum phase transitions on physical behavior, especially their role in stabilizing novel electronic phases. Much experimental and theoretical attention has focussed on magnetically ordered metals, and the heavy electron compounds have been especially heavily studied due to their electronic and behavioral diversity, as well as the proven utility of the Doniach phase diagram as an organizational scheme for the entire class of materials [1]. Many magnetically ordered heavy electron compounds have been studied, where both antiferromagnetic and ferromagnetic transitions have been suppressed to form magnetic quantum critical points [2]. Nonetheless, the need to make a link between experimental results and theoretical models place considerable constraints on experimental systems. Ideally, such compounds should be single crystals of stoichiometric compounds, demonstrated to have low levels of disorder. As grown, magnetic order should occur at the lowest possible temperatures, but continuous variables such as pressure or magnetic fields can be used to tune the system to the quantum critical point. Tuning criticality using compositional variation is to be avoided if at all possible, due to the profound impact which disorder has been demonstrated to have on some quantum critical systems. For these reasons, most attention has focussed on a few model systems such as $YbRh_2Si_2$ [3], $Sr_3Ru_2O_7$ [4], and $CeCu_{6-x}Au_x$ [5]. It is clear that in order to make continued progress towards exploring and refining the available theoretical models, new quantum critical systems must be identified which not only have diverse magnetic properties, but also satisfy most—if not all—of these stringent criteria. We report here the synthesis and essential properties of a new intermetallic antiferromagnet, Yb_3Pt_4, which has great promise as a host for quantum criticality.

2. Experimental details

Single-crystalline samples of Yb_3Pt_4 were grown using a Pb flux [6]. Equal molar amounts of Yb and Pt were dissolved in

* Corresponding author at: Department of Physics, University of Michigan, Ann Arbor, MI 48109-1120, USA.
E-mail address: mcbennet@umich.edu (M.C. Bennett).

molten Pb in an alumina crucible, by heating the mixture of elements to 1200 °C in vacuum in a sealed quartz tube. The mixture was then cooled slowly to 450 °C, resulting in the formation of crystals. Molten Pb was removed by centrifuging the crucible, isolating the single crystals, which have typical dimensions of $0.2 \times 0.2 \times 1 \, mm^3$. The crystals were etched in a 50/50 by volume mixture of acetic acid and hydrogen peroxide to remove any traces of the Pb flux remaining on the surface. Single crystal X-ray diffraction measurements of a fragment of one of the measured crystals determined that Yb_3Pt_4, crystallizes in a rhombohedral $hR14$ (No. 148) space group with lattice parameters of $a = 12.8971 \, Å$, $c = 5.6345 \, Å$, and $V = 811.65 \, Å^3$, with $Z = 6$. Yb_3Pt_4 is a known compound [7], but single crystals have not previously been synthesized. Single crystals of a similar compound, Yb_3Pd_4, have been grown and measured [8,9] and share the same rhombohedral crystal structure and several of the physical properties of Yb_3Pt_4, but this is the first report of the physical properties of Yb_3Pt_4, either polycrystalline or single crystal. The structure was solved and refined using the SHELXL-97 program [10]. Corrections were made for absorption and extinction, and the atomic positions were refined with anisotropic displacement parameters. Atomic coordinates and thermal parameters are listed in Table 1. The primitive cell is quite simple with three Pt positions, and just one Yb position. The full unit cell contains 18 Yb atoms, and 24 Pt atoms as illustrated in Fig. 1a, along with the polyhedra for each atomic position. The Pt1 and Pt3 positions haveoctahedral coordination, and the Pt2 and Yb4 sites show irregular polyhedral coordination. Fig. 1b is a schematic of a section of a Yb_3Pt_4 single crystal consisting of eight unit cells, and shows a structure of alternating layers of Yb and Pt.

The electrical resistivity was measured in a quantum design physical property measurement system (PPMS) using a conventional four-probe method between 0.4 and 300 K in zero field and in magnetic fields as large as 9 T. Contacts were made to the crystal using silver epoxy, which was cured at 100 °C for several hours. Contact resistances typically ranged from 1 to 10 Ω. To determine the resistance of the Yb_3Pt_4 crystal, an alternating current is driven through the crystal at 7.5 Hz, with amplitudes ranging from 100 to 500 µA and the resulting voltage drop across the crystal is measured. Magnetization measurements were performed using a quantum design magnetic property measurement system (MPMS), at temperatures ranging from 1.8 to 300 K, and in magnetic fields up to 7 T. AC magnetic susceptibility measurements were also performed in the MPMS, using a 17 Hz AC field with an amplitude of 4.17 Oe. Specific heat measurements were performed using a PPMS for temperatures between 0.4 and 70 K.

3. Results and discussion

The magnetic properties of Yb_3Pt_4 indicate that this compound has local moment character at high temperatures. The magnetic susceptibility measured with a field of 0.2 T parallel ($\chi_\parallel$) and perpendicular ($\chi_\perp$) to the c-axis is plotted in Fig. 2a. The

Table 1
Crystallographic data for Yb_3Pt_4.

Atom	Site	x	y	z	U_{eq}[a]$(Å^2)$
Pt1	$3a$	0	0	0	0.00754
Pt2	$18f$	0.88391	0.28131	0.05311	0.00534
Pt3	$3b$	0	0	1/2	0.00975
Yb	$18f$	0.04279	0.21182	0.23494	0.00630

[a] U_{eq} is defined as one-third of the trace of the orthogonalized U_{ij} tensor.
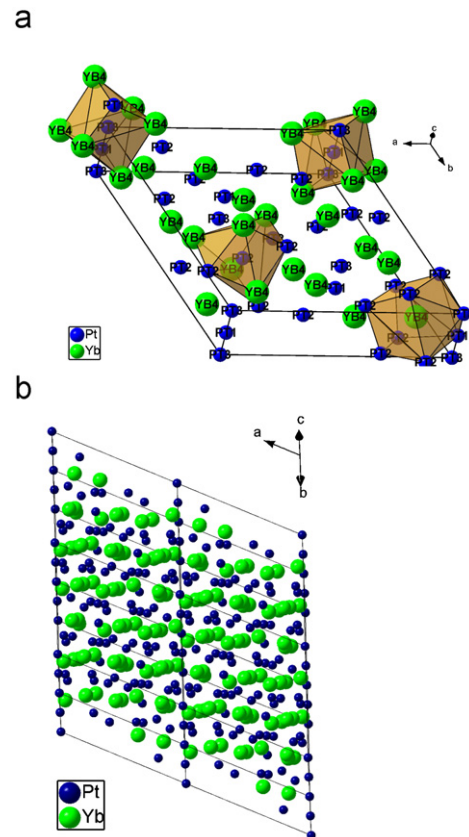

Fig. 1. (a) Schematic representation of the unit cell and the polyhedra associated with each atomic site of Yb_3Pt_4 crystallizing in the rhombohedral $hR14$ (No. 148) structure. There are 18 Yb and 24 Pt atoms in the unit cell of Yb_3Pt_4. The Pt atoms are represented by the blue (dark gray) spheres, and the Yb atoms are represented by the green (gray) spheres, as indicated in the key. (b) Schematic of a section of a single crystal of Yb_3Pt_4 showing the layering of Yb and Pt atoms within the structure. Eight unit cells are shown. (For interpretation of the reference to color in this figure legend, the reader is referred to the web version of this article.)

susceptibilities increase smoothly with decreasing temperature, and as indicated in the inset to Fig. 2a, the anisotropy $\chi_\parallel/\chi_\perp$ is near unity throughout the high temperature local moment regime, and reaches a maximum value slightly larger than two below ~150 K.

The inverses of $\chi_\parallel$ and $\chi_\perp$ are plotted as functions of temperature in Fig. 2b. The same Curie–Weiss behavior is found above ~150 K for both field orientations, where $\chi_{\parallel,\perp} = C/(T + \theta)$. The effective moment per Yb ion, deduced from the Curie constant $C = \mu_{eff}^2/3k_B$, where the effective magnetic moment per Yb ion, $\mu_{eff} = g\mu_B\sqrt{J(J+1)}$ is 4.24 μ_B, which is just below Hund's rule moment for Yb^{3+}, 4.54 μ_B. We find that the Weiss temperature $\theta = -2.3$ K, indicating net antiferromagnetic interactions among the Yb moments. Curie–Weiss behavior is observed down to the lowest temperatures for $\chi_\perp$, although $1/\chi_\parallel$ is slightly enhanced above the Curie–Weiss law for temperatures below ~150 K. This may result from the depopulation of the full Yb^{3+} crystal field manifold, presumed to be fully occupied for temperatures above ~150 K. The susceptibility data indicate that the easy axis for the local Yb moments is perpendicular to the c-axis at low temperatures.

Further evidence for the local moment character of Yb_3Pt_4 comes from magnetization measurements, which have been carried out at a variety of temperatures between 2 and 100 K (Fig. 3a), with the fields applied perpendicular to the c-axis. At high temperatures, the magnetization M is linear with field H, but a pronounced curvature develops as the temperature is reduced.
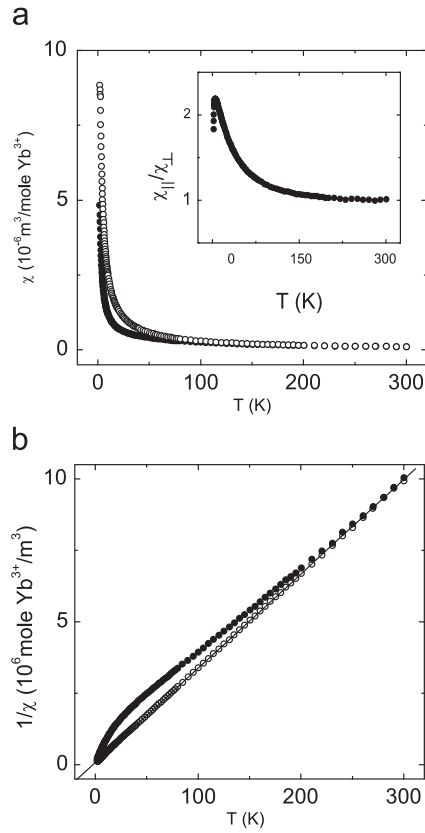
Fig. 2. (a) The temperature dependence of the magnetic susceptibility of Yb_3Pt_4 with a 0.2 T field parallel ($\chi_\parallel$, filled circles) and perpendicular ($\chi_\perp$, hollow circles) to the c-axis. The inset shows the magnetic anisotropy $\chi_\parallel/\chi_\perp$. (b) The inverses of $\chi_\parallel$ (filled circles) and $\chi_\perp$ (hollow circles) with a Curie–Weiss fit to the data for the perpendicular configuration (solid line).

Fig. 3. (a) The magnetic field H dependence of the magnetization of Yb_3Pt_4 at different temperatures T with H perpendicular to the c-axis. (b) Data from (a) plotted as a function of H/T. The $J = 7/2$ Brillouin function (solid line) compares unfavorably to the data.

Fig. 4. The temperature dependence of the magnetic and electronic heat capacity, C_M (solid line), and its associated entropy, S (dashed line). The dotted line indicates a fit to a Schottky expression, yielding peaks at 26 and 63 K.

These data have been replotted in Fig. 3b as functions of field divided by temperature, H/T. For all temperatures, the magnetization collapses on to a universal curve, as indicated in Fig. 3b, implying simple paramagnetic behavior. As we will show below, we believe that the crystal field split manifold of Yb^{3+} states is being thermally populated above ∼30 K, varying the effective Yb^{3+} moment for temperatures below ∼150 K, and indeed Fig. 3b shows that the high field magnetization does not approach the nominal $J = 7/2$, $g = 8/7$ high field value of $4\,\mu_B$/Yb at the lowest temperatures.

Measurements of the heat capacity, C, show that Yb_3Pt_4 becomes magnetically ordered at low temperature. We have estimated a phonon contribution C_{ph} to the total heat capacity C by fitting the high temperature $C(T)$ to the Debye model, yielding a Debye temperature $\theta_D = 180\,K$, consistent with the value $\theta_D = 177\,K$ obtained from determinations of the atomic displacement parameters [11,12] taken from single crystal X-ray diffraction measurements. Below ∼10 K, $C_{ph} = \beta T^3$, with $\beta = 0.0013\,J/mol\,K^4$. The temperature dependence of the resulting magnetic and electronic heat capacity $C_M = C - C_{ph}$ is plotted in Fig. 4. At low temperatures, C_M is dominated by a large and extremely sharp transition at 2.4 K. The entropy S calculated from these data approaches Rln2 above 2.4 K, indicating that the 2.4 K transition corresponds to the magnetic ordering of a well-isolated doublet ground state. S/R increases gradually from ln 2 to ln 4 by ∼50 K. Clear evidence for a Schottky peak at 26 K is seen in Fig. 4, and the Schottky fit implies that the first and second excited states have energies of 50 and 127 K. The temperature dependence of the entropy, S, is consistent with two crystal field split doublet states
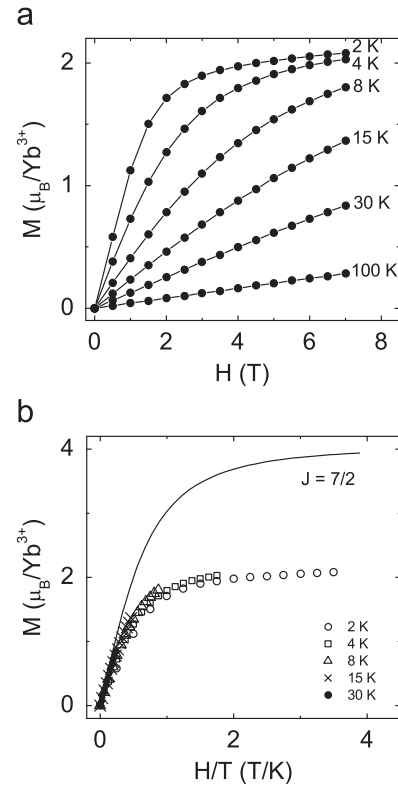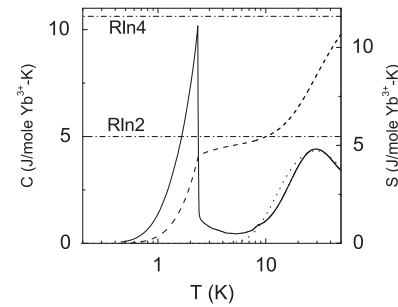
and one quartet state, as expected for Yb in a rhombohedral local environment [9].

An analysis of the raw specific heat data confirms that there is a latent heat associated with the transition (Fig. 5), showing that it is at least weakly first order. The heat capacity on each side of the transition is clearly separated into two linear regions on the semi-log plot, the larger sloped, lower heat capacity found above T_N, and the smaller sloped, higher heat capacity region found below T_N. For a second order phase transition, the two lines intersect at the critical temperature. However, for a first order transition, the associated latent heat results in an apparent decrease in the cooling rate near the transition temperature. This effect is evident in Fig. 5.

Taking known values for the thermal conductance between the crystal and the thermal bath, the measured change in temperature during the heat pulse, and knowing from the plot in Fig. 5 that the undercooling effect is present for ∼3.5 s, we estimate an upper
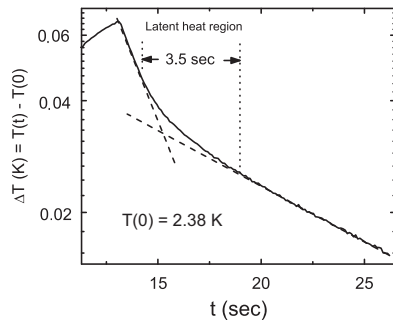
Fig. 5. A semi-log plot of the time dependence of the temperature of the crystal during a heat capacity measurement near the phase transition at 2.38 K. The non-linear region is associated with a latent heat, as described in the text.

Table 2
Latent heats and critical temperatures of first order ferromagnetic or antiferromagnetic transitions in some rare earth elements, and rare earth based compounds.

Compound	T_C (K), T_N (K)	L (J/mol RE)	Ref.
Dy	91(FM)	39	[13]
Er	19(FM)	24	[14]
$Er_{0.4}Ho_{0.6}Rh_4B_4$	1.9(FM)	74.5	[15]
Sm_2IrIn_8	14(AFM)	5	[16]
$Sm_{0.55}Sr_{0.45}MnO_3$	130(FM)	180	[17]
Yb_3Pt_4	2.4(AFM)	0.09	This work

bound for the latent heat to be 2×10^{-4} J/g, or 0.09 J/mol-Yb. Table 2 is a list of the latent heats and magnetic ordering temperatures for some rare earth elements and rare earth based magnetic compounds that have first order ferromagnetic and antiferromagnetic transitions. The latent heat of Yb_3Pt_4 is two to three orders of magnitude lower than those found in these rare earth based magnetic compounds, indicating that this transition is very weakly first order.

Measurements of the ac magnetic susceptibility χ' show that Yb_3Pt_4 likely orders antiferromagnetically in zero field. As shown in Fig. 6a, the real part of χ' has a distinct cusp, corresponding to a discontinuity in the temperature derivative $d\chi'/dT$ at 2.4 K, the temperature where the ordering transition is observed in the heat capacity, C_M. As indicated in Fig. 6b, the antiferromagnetic transition is revealed as a marked slope change at 2.4 K for the dc susceptibilities $\chi_\perp^{-1}$ and $\chi_\parallel^{-1}$, showing that the antiferromagnetic order develops directly from a simple paramagnetic state without appreciable critical fluctuations or substantial magnetic anisotropy. Fig. 6b shows that the dominant component of the susceptibility in the magnetically ordered state is large and temperature independent, approaching a value of $\chi_\perp(0) = 6.8 \times 10^{-6}$ m³/mol Yb, and $\chi_\parallel(0) = 3.2 \times 10^{-6}$ m³/mol Yb.

The temperature dependence of the electrical resistivity $\rho(T)$ demonstrated in Fig. 7a indicates that Yb_3Pt_4 is a good metal. $\rho(T)$ decreases from the room temperature value of 108 μΩ cm to a residual value of ∼21 μΩ cm at 0.4 K. $\rho(T)$ has a broad maximum near 2.4 K, but drops by ∼25% with the onset of magnetic order. As is evident from Fig. 7b, the temperature dependences of the heat capacity and the temperature derivative of the resistivity $\partial\rho/\partial T$ are nearly identical, indicating that the resistivity is controlled both above and below T_N by fluctuations in the magnetization [18]. Application of a 9 T field (Fig. 7a inset) completely suppresses this spin disorder scattering, and renders the underlying resistivity linear in temperature from 0.4 to 40 K.

Our measurements indicate that the antiferromagnetically ordered state is a Fermi liquid, albeit one with unusual properties.
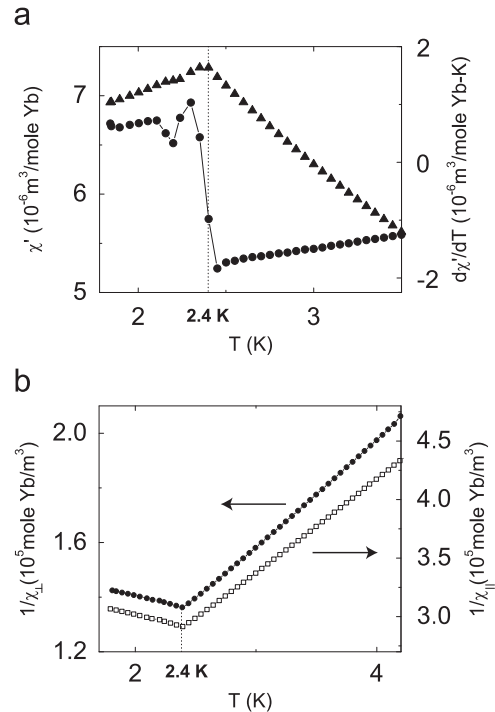

Fig. 6. The temperature dependence of the real part of the zero field ac susceptibility χ', showing an antiferromagnetic cusp and a discontinuity in its temperature derivative, $d\chi'/dT$ at the antiferromagnetic transition temperature, 2.4 K. (b) Clear changes in slope are found for $\chi_\perp^{-1}$ and $\chi_\parallel^{-1}$ at 2.4 K, although Curie–Weiss behavior is found down to the Neel temperature. The measuring field is 0.2 T.

We have plotted the temperature dependence of C/T in Fig. 8, along with several candidate fits. It is clear that there is little evidence for a quasiparticle contribution to the heat capacity $\gamma = C/T$. Spin wave expressions for C are compared to the data in Fig. 8. Despite the bulk antiferromagnetic order observed in the magnetic susceptibility measurements, C/T is poorly described by $C/T = T^2 \exp(-\Delta/k_B T)$, while reasonable agreement is found for the expression corresponding to ferromagnetic spin waves $C/T = T^{0.5} \exp(-\Delta/k_B T)$ with an anisotropy gap $\Delta = 1.2$ K. This may suggest that magnetic order in Yb_3Pt_4 results from the competition between both ferromagnetic and antiferromagnetic interactions. We note, however, that the gradual increase in C/T above T_N and the T^2 behavior found at the lowest temperatures may be consistent with an underlying Schottky peak, implying that the lowest lying Yb doublet may be split by ∼1.6 K, perhaps by the exchange interaction. Further experiments, such as measurements of the heat capacity in field, would be needed to test this possibility. In either case, the vanishingly small value of C/T found at the lowest temperatures suggests that the magnetic excitations which lead to the heat capacity in the ordered state are gapped. Seemingly, this would rule out the possibility that the ordered state is a Fermi liquid.

Given this conclusion, it is surprising that the electrical resistivity gives unambiguous evidence for Fermi liquid behavior in the antiferromagnetically ordered state. Fig. 9 shows that $\rho = \rho_0 + AT^2$ for temperatures smaller than the magnetic ordering temperature $T_N = 2.4$ K, with $\rho_0 = 21$ μΩ cm, and $A = 1.69 \times 10^{-6}$ Ω cm/K². This result shows that a substantial portion of the resistivity in the antiferromagnetic state results from quasiparticle scattering in a Fermi liquid, indicating that the relatively large resistivity does not result from strong impurity scattering but is an intrinsic feature of Yb_3Pt_4. The magnitude A of the quadratic resistivity is very large, comparable to values found in heavy electron systems such as UPt_3 [22–24]. Since the heat
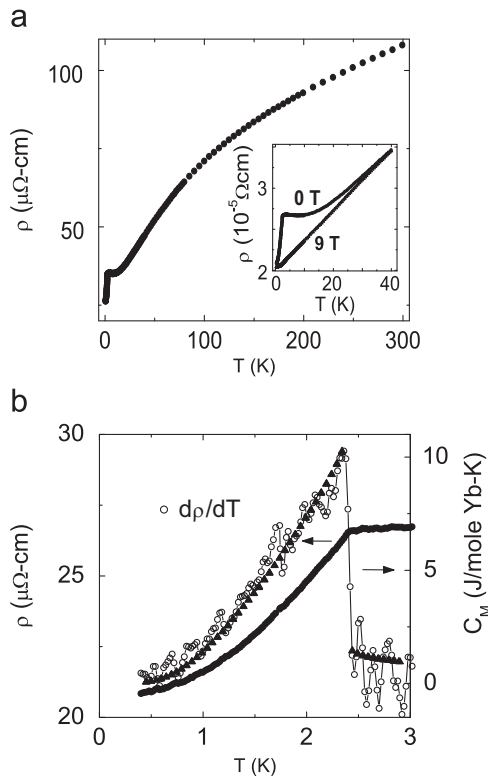
a

b

Fig. 7. (a) The temperature dependence of the electrical resistivity $\rho(T)$ of Yb_3Pt_4. Inset shows an expanded view of the low temperature resistivity, in zero field and in a magnetic field of 9 T applied along the *c*-axis. (b) A comparison of the temperature dependences of C_M (filled triangles), the electrical resistivity ρ (filled circles), and the temperature derivative of the resistivity $\partial\rho/\partial T$ (open circles) near the antiferromagnetic transition temperature, $T_N = 2.4$ K.
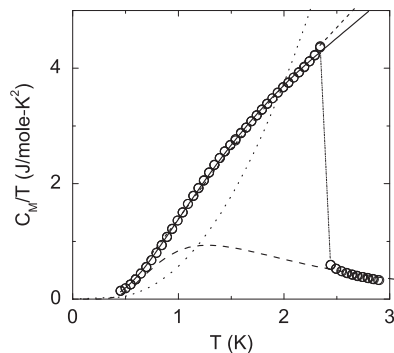

Fig. 8. The temperature dependence of the electronic and magnetic parts of the specific heat C_M divided by temperature (open circles) is fit to the expression for a ferromagnetic spin wave with a gap Δ (short-dashed line), $C_M/T = AT^{0.5}\exp^{-\delta/T}$, where $A = 3.3$ J/mol-Yb-$K^{5/2}$, and $\delta = \Delta/k_B = 1.2$ K. The dotted line is a fit to an antiferromagnetic spin wave, $C_M/T = AT^2\exp^{-\delta/T}$, assuming a 1 K gap. In both cases, the coefficient of the electronic part of the specific heat, γ is found to be negligible. The best fit to the data in the ordered phase is by $C_M/T = AT^0 e^{-\delta/T}$ (solid line). The dashed line is the expected Schottky anomaly if the doublet ground state is split.

capacity measurements rule out the presence of large numbers of massive quasiparticles, we conclude that the large Fermi liquid resistivity instead implies that there is a significantly reduced number of quasiparticles in Yb_3Pt_4. We can roughly estimate this number by assuming that the scattering rate per quasiparticle is the same in Yb_3Pt_4 as in other Yb-based heavy electron systems, i.e. that it has the same Kadowaki–Woods ratio $A/\gamma^2 = 1\,\mu\Omega\,cm\,mol^2\,K^2/J^2$ [23–25]. Since our heat capacity measurements place an upper bound on γ of 10 mJ/mol K^2, this implies
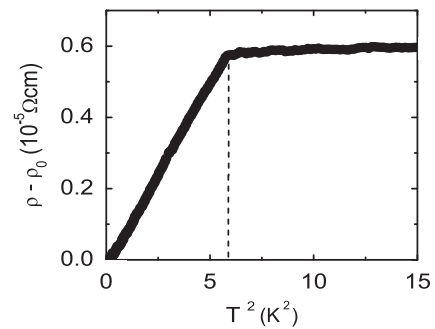

Fig. 9. The temperature dependent part of the electrical resistivity $\Delta\rho = \rho - \rho_0$ is quadratic in temperature below $T_N = 2.4$ K (dashed line).

that the number of quasiparticles per Yb is approximately 10^{-3}. Electronic structure calculations are needed to confirm this hypothesis.

The antiferromagnetically ordered state is characterized by an extremely large magnetic susceptibility. Fig. 6a shows that the ac susceptibility in the ordered phase has a temperature independent component which extrapolates to $6.8 \times 10^{-6}\,m^3$/mol-Yb. The temperature independence of this susceptibility suggests that it may be the Pauli susceptibility of a Fermi liquid. However, we note that this is a very large value, similar to those found in heavy electron systems, both in absolute terms and especially when weighted per quasiparticle. The Sommerfeld–Wilson ratio $R_W = \pi^2 k_B^2 \chi_0 / \mu_{eff}^2 \gamma$ is a useful figure of merit for judging the strength of ferromagnetic correlations within a Fermi Liquid. Most heavy electron compounds have R_W somewhat larger than the Kondo value of 2 [26,27]. Systems with ferromagnetic enhancement can have significantly larger values of R_W, such as Pd, where $R_W = 6-8$ [28], YbAgGe, where $R_W = 2$ [29], $YbRh_2Si_2$ where $R_W = 13$ [30], and also $Sr_3Ru_2O_7$ where $R_W = 10$ [31] The magnitude of the zero temperature susceptibility in Yb_3Pt_4 is comparable to those of the most enhanced heavy electron compounds [27]. although the Sommerfeld coefficient γ is several orders of magnitude smaller, implying an unreasonably large value for $R_W \sim 3600$. We believe that a more likely scenario is that, like the heat capacity, the temperature dependence of the ac susceptibility is dominated by fluctuations of presumably localized Yb moments and not the Pauli susceptibility of the few quasiparticles which provide the electrical resistivity.

Finally, it is worth noting that measurements have been performed on polycrystalline samples of the isostructural compound Yb_3Pd_4 which have some similarity to the results reported here for Yb_3Pt_4. Magnetic order is found in Yb_3Pd_4 at 3 K [8], and strong critical scattering is observed in inelastic neutron scattering measurements [9]. Magnetic susceptibility and X-ray absorption measurements [8] find that this compound is—unlike Yb_3Pt_4—significantly mixed valent. It might be interesting to explore this system more thoroughly, in particularly to see whether this mixed valent character could be suppressed by pressure, providing a direct connection to Yb_3Pt_4.

4. Conclusion

The picture which emerges from our measurements on the new compound Yb_3Pt_4 is that this is system which orders overall antiferromagnetically, with very little magnetic anisotropy. The transition is weakly first order, and there is little indication of critical fluctuations in either the magnetic susceptibility or the heat capacity. The large magnitude of the low temperature magnetic susceptibility, the observation of a Fisher–Langer

relation between the heat capacity and the temperature derivative of the resistivity, as well as the anisotropy gap found in the ordered phase heat capacity all suggest that the magnetic structure has a net ferromagnetic component as well. A possible explanation might be that the ground state of Yb_3Pt_4 involves a long-wavelength ferromagnetic modulation of the antiferromagnetic state similar to that found in the helical ferromagnet MnSi [32]. The temperature dependence of the heat capacity and the magnitude of the magnetic susceptibility together indicate that the localized moments continue to be an important part of the physics of the ordered phase.

The most remarkable of our findings is that magnetic order enables the formation of a Fermi liquid state in Yb_3Pt_4. Antiferromagnetic order emerges from a paramagnetic state involving fluctuations of individual Yb moments, and there is little evidence that the apparently localized moments are strongly coupled to conduction electrons via the Kondo effect, as they are in quantum critical systems such as the heavy electron compounds. The electrical resistivity is large for this class of intermetallics, both in the paramagnetic and ordered phases. However, the substantial loss of spin-disorder scattering associated with the magnetic transition indicates that low carrier density and not strong impurity scattering is likely the primary source of this high but decidedly metallic resistivity. Given this apparent weak coupling between the magnetic moments and the conduction electrons, it is somewhat surprising to find that the resistivity in the ordered state is that of a Fermi liquid: quadratic with temperature $\rho(T) = \rho_0 + AT^2$, and with a coefficient A as large as those found in heavy electron compounds. The absence of a large quasiparticle contribution to the heat capacity subsequently implies that the Fermi surface in the ordered phase has a small volume, perhaps consisting of isolated pockets.

The central issues surrounding the suitability of an ordering material as an eventual host for quantum criticality are the classification of the phase transition, with respect to order and mechanism, and the ways in which the underlying electronic structure is affected by the onset of magnetic order. While we know that the magnetic ordering phase transition is dominantly antiferromagnetic and weakly first order, the overall classification of the phase transition in Yb_3Pt_4 into local moment type or Fermi surface instability is not wholly settled by our experiments. On the one hand, spin wave expressions provide a reasonable description of the ordered phase heat capacity, however, the magnitude of the magnetic susceptibility is much too large to be conveniently assigned to itinerant Fermi surface states. In the local moment ordering scenario, superzone formation can potentially gap the Fermi surface, although the low crystal symmetry of Yb_3Pt_4 suggests that this gapping would be at best partial. The large value of the quasiparticle resistivity is consistent with the formation of a Fermi liquid comprised the few states at the Fermi energy which survive this gapping. While it would be quite important to know whether these quasiparticles have substantial mass enhancement, a definitive determination would require knowing the quasiparticle contributions to the magnetic susceptibility and heat capacity, which are apparently masked by the larger local moment contributions. However, the onset of Fermi liquid behavior exactly at the Neel temperature suggests that antiferromagnetic order involves a more profound modification to the Fermi surface and its excitations than is afforded by

simple superzone formation. We cannot rule out the possibility that a Fermi surface instability plays a role in driving magnetic order in Yb_3Pt_4. More information about the magnetic structure and dynamics in the ordered state, as well as direct determinations of the Fermi surface above and below the transition are needed to provide a definitive resolution of this issue.

Acknowledgments

References

[1] S. Doniach, in: R.D. Parks (Ed.), Valence Instabilities and Related Narrow Band Phenomena, Plenum, New York, 1977, p. 169.
[2] G.R. Stewart, Rev. Mod. Phys. 73 (2001) 797.
[3] P. Gegenwart, J. Custers, C. Geibel, K. Neumaier, T. Tayama, K. Tenya, O. Trovarelli, F. Steglich, Phys. Rev. Lett. 89 (2002) 056402.
[4] S.A. Grigera, P. Gegenwart, R.A. Borzi, F. Weickert, A.J. Schofeld, R.S. Perry, T. Tayama, T. Sakakibaram, Y. Maeno, A.G. Green, A.P. Mackenzie, Science 306 (2004) 1154.
[5] H. von Lohneysen, J. Phys. Condens. Matter 8 (1996) 9689.
[6] Z. Fisk, J.P. Remeika, in: K.A. Gschneidner, L. Eyring (Eds.), Handbook on the Physics and Chemistry of the Rare Earths, vol. 12, Elsevier Science Publishers B.V., 1989, p. 53.
[7] A. Palenzona, J. Less-Common Metals 53 (1977) 133.
[8] B. Politt, D. Durkop, P. Weidner, J. Magn. Magn. Mater. 47&48 (1985) 583–585.
[9] U. Walter, D. Wohlleben, Phys. Rev. B 35 (1987) 3576.
[10] G.M. Sheldrick, SHELXL-97, Program for Crystal Structure Refinement, University of Göttingen, Germany, 1997.
[11] B.C. Sales, D.G. Mandrus, B.C. Chakoumakos, in: Recent Trends in Thermoelectric Materials Research II, Academic Press, San Diego, California, 2000, p. 1.
[12] B.C. Sales, B.C. Chakoumakos, D. Mandrus, J.W. Sharp, J. Solid State Chem. 146 (1999) 528–532.
[13] K.D. Jayasuriya, S.J. Campbell, A.M. Stewart, Phys. Rev. B 31 (9) (1985) 6032.
[14] C.S. Durfee, C.P. Flynn, Phys. Rev. Lett. 87 (5) (2001) 057202-1.
[15] B. Lachal, M. Ishikawa, A. Junod, J. Muller, J. Low Temp. Phys. 46 (5/6) (1982) 467.
[16] P.G. Pagliuso, J.D. Thompson, M.F. Hundley, J.L. Sarrao, Z. Fisk, Phys. Rev. B 63 (2001) 054426.
[17] A.S. Chernyshov, M.I. Ilyn, A.M. Tishin, O.Yu. Gorbenko, V.A. Amelichev, S.N. Mudretsova, A.F. Mairova, Y.I. Spichkin, Cryocoolers 13 (2004) 381.
[18] M.E. Fisher, J.S. Langer, Phys. Rev. Lett. 20 (1968) 665;
S. Alexander, J.S. Helman, I. Balberg, Phys. Rev. B 13 (1976) 304.
[22] A. de Visser, J.J.M. Franse, A. Menovsky, J. Magn. Magn. Mater. 43 (1984) 43.
[23] K. Kadowaki, S.B. Woods, Solid State Commun. 58 (1986) 507.
[24] N. Tsujii, K. Yoshimura, K. Kosuge, J. Phys. Condens. Matter 15 (2003) 1993.
[25] H. Kontani, J. Phys. Soc. Jpn. 73 (2004) 515.
[26] A.C. Hewson, The Kondo Problem to Heavy Fermions, Cambridge University Press, Cambridge, 1993, p. 15.
[27] Z. Fisk, H.R. Ott, G. Aeppli, Jpn. J. Appl. Phys. 26 (26-3) (1987) 1882.
[28] F.M. Mueller, A.J. Freeman, J.O. Dimmock, J.M. Furdyna, Phys. Rev. B (1) (1970) 4617.
[29] Y. Tokiwa, A. Pikul, P. Gegenwart, F. Steglich, S.L. Bud'ko, P.C. Canfield, Phys. Rev. B 73 (2006) 094435.
[30] P. Gegenwart, J. Custers, Y. Tokiwa, C. Geibel, F. Steglich, Phys. Rev. Lett. 94 (2005) 076402.
[31] S.-I. Ikeda, Y. Maeno, S. Nakatsuji, M. Kosaka, Y. Uwatoko, Phys. Rev. B 62 (2000) R6089.
[32] C. Pfleiderer, D. Reznik, L. Pintschorius, H.V. Lohneysen, M. Garst, A. Rosch, Nature 427 (2004) 227.